

Controlling Rashba spin splitting in Au(111) surface states through electric field

Shi-Jing Gong,^{1,2} Chun-Gang Duan,^{1,2,*} Yan Zhu,³ Zi-Qiang Zhu,¹ and Jun-Hao Chu^{1,2}

¹Key Laboratory of Polar Materials and Devices, Ministry of Education, East China Normal University, Shanghai 200062, China

²National Laboratory for Infrared Physics, Chinese Academy of Sciences, Shanghai 200083, China

³College of Science, Nanjing University of Aeronautics and Astronautics, Nanjing 210016, China

(Received 27 August 2012; revised manuscript received 19 October 2012; published 2 January 2013)

Combining density-functional theory (DFT) calculations and theoretical analyses, we demonstrate the high-order Rashba spin-orbit coupling in the Au(111) surface and the electric field manipulation of the Rashba splitting energy. A good linear relationship between the Rashba splitting energy and applied electric field is revealed by DFT calculations. The effect is attributed to the linear response of the first-order Rashba parameter to the applied electric field. The nonlinear relationship between Rashba splitting energy and the wave vectors identifies the higher-order Rashba components, which, however, are found to be less influenced by the external electric field. Our investigation provides an in-depth understanding of the tunability of Rashba splitting in a metal surface, which is of great interest in the area of electrical control of spin states.

DOI: 10.1103/PhysRevB.87.035403

PACS number(s): 73.20.At, 71.70.Ej, 79.60.Dp

I. INTRODUCTION

Spin-orbit coupling (SOC), which acts as a bridge between the orbital motion and the spin degree of freedom, is winning growing research interest fueled by its potential applications in future nanoelectronics.^{1–3} Various SOC-dependent spintronic devices, such as spin field-effect-transistors,⁴ spin interferences,⁵ and spin filters,^{6,7} etc., have been proposed, and some have been experimentally confirmed. Meanwhile, many interesting physical phenomena, including the topological insulator,⁸ the spin-Hall effect,⁹ and the magnetic anisotropy,¹⁰ are found to be related to SOC.

Among various kinds of spin-orbit couplings, Rashba-type SOC³ attracts the most attention due to its tunability through an external electric field, which has been experimentally implemented in semiconductor heterostructures.¹¹ Metal surfaces^{12–16} form a new family for investigation of Rashba SOC. Research interest in metal surface begins with the Au(111) surface, in which a considerable Rashba spin splitting, about 110 meV at the Fermi level, was obtained in the *sp*-derived surface states through angle-resolved photoelectron spectroscopy,¹² and very recently a giant room-temperature spin-Hall effect was observed due to surface-assisted skew scattering.¹⁷ Subsequently, similar investigations were carried out for other metal surfaces, such as Bi(111),¹⁴ Ir(111),¹⁵ Gd(0001),¹⁶ etc. Recent studies have extended to surface alloys, such as Ag/Au(111),¹⁸ Ag/Pt(111),¹⁹ Bi/Ag(111),²⁰ etc., aiming to tune the magnitude of the Rashba splitting strength by surface modification. The electric field, the most promising and popular approach to tune Rashba SOC strength in semiconductor heterostructures, however, is seldom exploited in the metal surfaces. Bihlmayer *et al.* were the first group to try the electric field control of Rashba splitting at a metal surface, yet they just provided very simple discussions.²¹ Very recently, Park *et al.* calculated the Rashba splitting in a single Bi layer under an external electric field, and the obtained results verified their new theoretical model about the formation of the Rashba surface band splitting.²² A single metal layer itself, however, shows no inversion asymmetry, and thus an extremely strong electric field is required to produce considerable Rashba splitting, which may be of little

practical significance. Therefore, more detailed calculations and in-depth analyses about the influence of electric field on Rashba splitting at a metal surface are in urgent demand, which forms the motivation of our present work.

In our previous study, we investigated the influence of the electric field on surface magnetic anisotropy of 3*d*-transitional metal films,²³ in which the Rashba effect is very weak and therefore ignored. Now we concentrate on the electric field manipulation of the Rashba spin splitting in Au(111) surface states. The electric-field-induced surface dipoles, and the variation in the electrostatic potential distribution and the Rashba splitting energy are discussed in detail. Our findings are of considerable interest in electrically controlled magnetism, and may also provide an alternative tactic to manipulate the room-temperature spin-Hall effect observed in Au(111) surfaces.¹⁷

II. METHOD OF CALCULATION

The calculations are performed within density-functional theory (DFT) using the projector-augmented wave (PAW) method implemented in the Vienna *Ab-initio* Simulation Package (VASP).²⁴ The exchange-correlation potential is treated in the local-spin-density approximation, with SOC included. We use the energy cutoff of 400 eV for the plane wave expansion of the PAWs and a $37 \times 37 \times 1$ Γ centered *k*-point grid in the self-consistent calculations. For geometry optimization, all the internal coordinates are relaxed until the Hellmann-Feynman forces are less than 1 meV/Å. The Au surfaces are simulated using a slab model, in which a large enough vacuum thickness (20 Å) along the *z* axis is adopted to avoid the interaction between adjacent supercells.

III. RESULTS AND DISCUSSION

We first check Rashba spin splitting of the freestanding Au(111) slab with surface lattice constant 2.88 Å.²⁵ Figure 1(a) shows the Rashba splitting bands of a 22-layer Au(111) slab, which is thick enough to prevent the interaction between the two surfaces of the slab and produces the saturated Rashba spin splitting energy.²⁶ It is clear that the Rashba splitting bands are around -0.4 eV below the Fermi level at the Γ

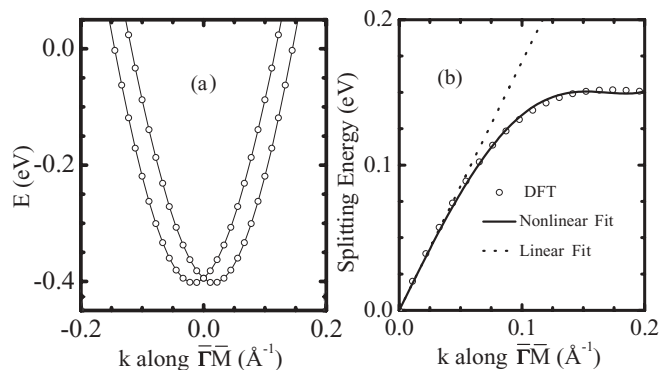


FIG. 1. (a) Rashba splitting bands of 22-layer Au(111) along $\bar{\Gamma}\bar{M}$. (b) Rashba splitting energy versus the wave vector, where open circles indicate the DFT results, and dotted and solid lines display linear and fifth-order fits as described in the text.

point, and the spin splitting energy is more than 100 meV, agreeing well with previous reports.^{11,12} Figure 1(b) shows the Rashba splitting energy versus the wave vector, in which the open circles represent the DFT results, and dotted and solid lines are the linear (first-order) and nonlinear fits, respectively. As can be clearly seen, when the wave vector becomes large ($k > 0.05 \text{ \AA}^{-1}$), the Rashba splitting energy deviates from the linear relation with wave vector, and the higher-order Rashba contribution²⁷ is required for a good fit.

Note that the higher-order Rashba contributions in the Au(111) surface have not been discussed in previous investigations. Here, we provide details about them. Indeed, the higher-order Rashba components can be found in the general Rashba Hamiltonian:

$$H_{\text{soc}} = \frac{\hbar}{4m^2c^2} \left(1 - \frac{1}{4m^2c^2} p^2 + \frac{1}{16m^4c^4} p^4 \dots \right) (\nabla V \times \mathbf{p}) \cdot \boldsymbol{\sigma}, \quad (1)$$

where m is the effective mass of the electron, c is the speed of light, $\boldsymbol{\sigma}$ is the Pauli matrix, \mathbf{p} is the operator of the electron's momentum, and V is the effective one-electron potential energy. Here, ∇V is the gradient of the potential energy, which includes both the surface potential gradient and the potential gradient close to the nucleus of an atom.²¹ Note that the higher-order Rashba terms are significant only when the *velocity* of the electron is comparable with c , i.e., relativistic effect is strong. In general, this condition is only possible in the region of core electrons of high- Z (Z is the atomic number) atoms. For low- Z materials, the first-order Rashba component is enough to describe the relativistic correction. For example, the spin-Hall effect observed in GaAs semiconductors can be well described by the linear Rashba SOC.^{28,29} Even in GaAs, Yang *et al.* predicted the nonlinear Rashba contribution when the wave vector is large.³⁰ We name the latter two items in the right side of Eq. (1) to be the third- and fifth-order Rashba components, respectively, which will be used in our following discussion.

To well fit the Rashba splitting energy obtained by DFT calculations in a Au(111) surface, we find that the fifth-degree polynomial should be included. Using the fitting function ($\alpha_1 k + \alpha_3 k^3 + \alpha_5 k^5$), we get the parameters $\alpha_1 = 1.71 \text{ eV \AA}$, $\alpha_3 = -41.3 \text{ eV \AA}^3$, and $\alpha_5 = 431.1 \text{ eV \AA}^5$. The excellent agreement between the DFT calculations and the fifth-order

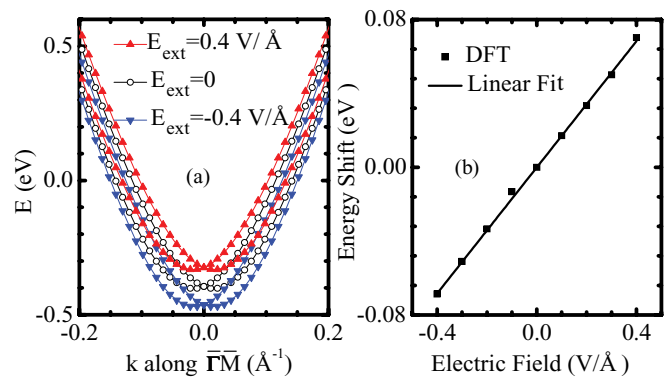


FIG. 2. (Color online) (a) The surface Rashba splitting bands under the electric fields $\mathbf{E}_{\text{ext}} = 0$ (open circles), 0.4 V/\AA (up-triangles), and -0.4 V/\AA (down-triangles). (b) Electric-field dependence of the band energy shift (squares). The solid line is a linear fit to the calculated data.

fit, shown in Fig. 1(b), identifies the contribution of the higher-order Rashba components and also substantiates the importance of the nonlinear Rashba components.

Next, we consider the influence of the imposed electric field on the freestanding Au(111) slab. A uniform electric field is applied perpendicular to the Au(111) surface. The approach used to handle electric field in VASP is the addition of an artificial dipole layer in the middle of the vacuum,³¹ which has been proved practical for metal surface.^{23,32} Whether the electric field can manipulate the Rashba spin splitting at a metal surface still remains unclear, and very few reports can be found.^{21,22} It is known that when an electric field is applied to a metal slab, it will induce screening charges at the metal surface and therefore modify the surface electrostatic potential.²³ At a magnetic metal surface, the screening effect is spin-dependent and can induce the surface magnetoelectric coupling effect, which has been illustrated in our previous work on the ferromagnetic thin films Fe(001), Ni(001), and Co(0001).²³ For these systems, however, due to their low atomic numbers, even the linear Rashba effect is very weak. Therefore, we do not expect large Rashba spin splittings in these systems, and the electric field effect on their spins is mainly due to spin-dependent screening at the surface. For nonmagnetic metals like Au, the screening effect shows no difference between spin-up and spin-down electrons, and consequently the Rashba SOC is the only known mechanism by which the external electric field could influence the spins.

Following the same strategy used in Ref. 23, we apply different magnitudes of external electric field on the Au(111) slab. The Rashba splitting bands under the electric fields $\mathbf{E}_{\text{ext}} = -0.4 \text{ V/\AA}$ and 0.4 V/\AA are shown in Fig. 2(a), in which the bands for $\mathbf{E}_{\text{ext}} = 0$ are also presented for a clear comparison. Here, a positive electric field is defined to be pointed away from the metal surface. The calculated data reveal that a positive (negative) electric field induces an upward (downward) shift of the splitting bands, as the consequence of the formation of induced surface dipoles. Figure 2(b) plots the electric-field dependence of band energy shift at the Γ point. The squares indicate the data obtained from DFT calculations, and the solid line is a linear fit to the calculated data. A good linear

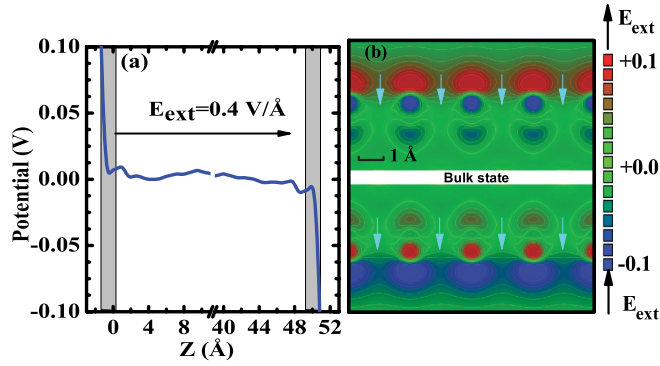


FIG. 3. (Color online) (a) The xy -plane averaged electrostatic potential induced by the electric field, $\Delta V_z = V(\mathbf{E}_{\text{ext}}) - V(0)$. Shaded area indicates the surface region. (b) Charge densities induced by the electric field, $\Delta\rho = \rho(\mathbf{E}_{\text{ext}}) - \rho(0)$, in arbitrary units. Down arrows in (b) indicate the induced surface dipoles to screen the external electric field.

relationship between the energy shift and the applied electric field is clearly observed.

To well understand the shift behavior discussed above, we show the electric-field-induced electrostatic potential and charge densities at the Au surface in Figs. 3(a) and 3(b), respectively. The steep potential at the two surfaces is clearly observed. The two shaded areas indicate the surface regions, which only include the surface Au atoms. It is clear that the electric-field-induced potentials ($\Delta V_z = V[\mathbf{E}_{\text{ext}}] - V[E = 0]$) for the two surfaces are opposite in sign. This electric-field-induced potential directly results in the shift of the Rashba splitting bands. As can be clearly seen in Fig. 3(a), when $E = 0.4 \text{ V/Å}$, ΔV_z for the surface electron approaches to 0.1 V, which is quantitatively consistent with the energy shift in Fig. 2(b). The induced screening dipoles are shown in Fig. 3(b), in which we just consider the outmost Au layer because the bulk states of the inner layers can hardly be influenced by the electric field. Down arrows in Fig. 3(b) denote the induced surface dipoles to screen the external electric field. We notice that the induced charge densities at the surfaces have a dumbbell shape, indicating the dominance of p_z orbitals in the surface states.

The external electric field not only shifts the Rashba splitting bands, but also changes the Rashba splitting energies. This is made possible by modifying the gradient of electrostatic potential in the Rashba Hamiltonian. To be specific, we write the first-order Rashba Hamiltonian as:

$$\begin{aligned} H_{\text{soc}}^1 &= \frac{\hbar}{4m^2c^2} [\nabla(V + V_{\text{ext}}) \times \mathbf{p}] \cdot \sigma \\ &= \frac{\hbar}{4m^2c^2} [(\nabla V - e\mathbf{E}_{\text{ext}}) \times \mathbf{p}] \cdot \sigma, \end{aligned} \quad (2)$$

where e is the charge of electron, and \mathbf{E}_{ext} stands for the external electric field. For the Au(111) surface, the gradient of the surface potential is along the z direction, and so the first-order Rashba parameter can be written as:

$$\alpha_1 = \frac{\hbar^2}{4m^2c^2} \left(\frac{\partial V}{\partial z} - eE_{\text{ext}} \right). \quad (3)$$

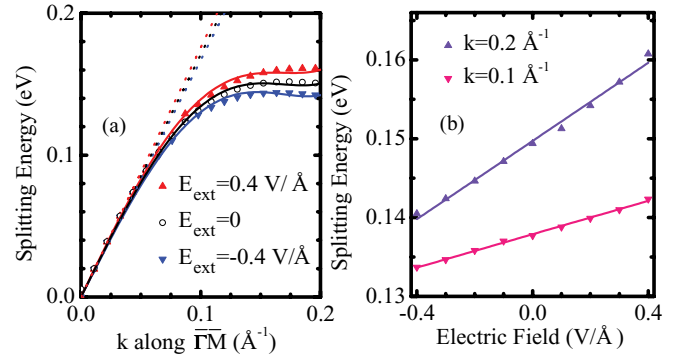


FIG. 4. (Color online) (a) Rashba splitting energies under the electric fields $\mathbf{E}_{\text{ext}} = 0$ (open circles), -0.4 V/Å (down-triangles), and 0.4 V/Å (up-triangles). Dotted and solid curves are the first-order and fifth-order fits as described in the text. (b) Rashba spin splitting energy versus the electric field, under the different wave vectors $k = 0.1 \text{ Å}^{-1}$ (down-triangles) and 0.2 Å^{-1} (up-triangles), where the solid lines are linear fits to the calculated data.

From Eq. (3), we can see that the increase of external electric field will enhance the effective electric field and thus the first-order Rashba parameter. As shown in Fig. 4(a), which depicts the Rashba splitting energies under various electric fields, the calculations do show such tendency, i.e., positive (negative) electric field enhances (suppresses) the splitting energy. Note that the order of the magnitude of potential gradient close to the nucleus is generally 10 V/Å , which is much larger than the electric field we apply on the slab. Therefore, the modification of the Rashba parameter is quite small. Indeed, the difference in splitting energy caused by the external electric field becomes noticeable only for large wave vectors [see Fig. 4(a)].

As we described previously, the higher-order Rashba components are important only for the strong relativistic effect. In our case, this happens in the region of core electrons of Au. As the external electric field is screened by outmost conduction electron clouds, we expect it will not affect the higher-order Rashba terms. This is confirmed by our fitting of the electric-field-included DFT calculations, also shown in Fig. 4(a), in which dotted and solid lines are the first-order and fifth-order fits to the calculated data. Similarly, the first-order fitting agrees well with calculations for small wave vectors, and the deviation for large wave vector addresses the importance of higher-order terms.

For the fifth-order fits, we have tried two methods. One is fixing the parameters α_3 and α_5 at values obtained in the $\mathbf{E}_{\text{ext}} = 0$ case, assuming that the imposed electric field only affects the first-order Rashba component for the reason we discussed above. The other is freeing these three parameters. For method I, we get $\alpha_1 = 1.76 \text{ eV Å}$ at $E = 0.4 \text{ V/Å}$ and $\alpha_1 = 1.66 \text{ eV Å}$ at $E = -0.4 \text{ V/Å}$. As can be seen in Fig. 4(a), the excellent agreements between the fittings (solid lines) and calculated results (symbols) support our analysis that external electric field has no or little influence on the higher-order Rashba terms. For method II, at $E = 0.4 \text{ V/Å}$, we get the Rashba parameters $\alpha_1 = 1.73 \text{ eV Å}$, $\alpha_3 = -39.2 \text{ eV Å}^3$, and $\alpha_5 = 401.3 \text{ eV Å}^5$, and for $E = -0.4 \text{ V/Å}$, $\alpha_1 = 1.69 \text{ eV Å}$, $\alpha_3 = -43.3 \text{ eV Å}^3$, and $\alpha_5 = 465.0 \text{ eV Å}^5$. Comparing with the

corresponding parameters at $\mathbf{E}_{\text{ext}} = 0$ (1.71, -41.3 , and 431.1 , respectively), we find that the modification of parameters α_3 and α_5 shows a different trend of change from that of α_1 . Such results are, however, by no means reasonable. This is because even if V_{ext} appears in the higher-order terms of Eq. (1) like it does in Eq. (2), it should increase instead of decrease the absolute values of the higher-order parameters, for a positive electric field.

To see more clearly the electric field effect on the Rashba splitting energy, we plot in Fig. 4(b) the electric field dependence of Rashba splitting energy for different wave vectors, i.e., $k = 0.1 \text{ \AA}^{-1}$ and 0.2 \AA^{-1} . Up-triangles and down-triangles are the DFT calculation results, and the solid lines are the linear fits to the calculated data. The splitting energy changes nearly linearly with the electric field, and the slope is linearly dependent on wave vector, agreeing well with Eqs. (2) and (3). The electric field effect on large wave vectors is significant. Specifically, when the electric field of 0.4 V/\AA switches from negative to positive, there is a change of about 13.1% in the Rashba splitting energy for $k = 0.2 \text{ \AA}^{-1}$. The magnitude of the applied electric field (i.e., the *external* surface potential gradient) is comparable to the *intrinsic* surface potential gradient (i.e., $\Phi/\lambda_F \sim 0.86 \text{ V/\AA}$, where Φ is work function, and λ_F is the Fermi wavelength³³) of an Au(111) surface, which supports the previous finding that the large Rashba splitting in Au(111) surface states is not determined by the surface potential gradient, which works

only indirectly via the asymmetry of the wave function in the core region.³³

IV. CONCLUSIONS

In summary, we have investigated the electric-field manipulation of the Rashba splitting in an Au(111) surface. The first-principles calculations show that the electric field can tune the Rashba splitting strength by modifying the gradient of the surface electrostatic potential. We consider the electric field ranging from -0.4 V/\AA to 0.4 V/\AA , and find a linear relationship between the Rashba splitting energy and the applied electric field. Although both the linear and higher-order Rashba components exist in Au(111) surface states, only the former is responsible for the electric-field manipulation. Our investigation is of considerable interest in the area of electrical control of spin state.

ACKNOWLEDGMENTS

This work was supported by the 973 Program No. 2013CB922300, National Natural Science Foundation (NSF) of China (Grant No. 11004211, 50832003, 61125403, 60990312, 61076060, 61006089), Program for Changjiang Scholars and Innovative Research Team (PCSIRT), New Century Excellent Talents (NCET), and Fundamental Research Funds for the central universities (ECNU). Computations were performed at computing center of East China Normal University.

*Corresponding author address: wxbdcg@gmail.com or cgduan@clpm.ecnu.edu.cn

¹R. Winkler, *Spin-Orbit Coupling Effects in Two-Dimensional Electron and Hole Systems* (Springer, Berlin; New York, 2003).

²G. Dresselhaus, *Phys. Rev.* **100**, 580 (1955).

³A. B. Yu and E. I. Rashba, *J. Phys. C: Solid State Phys.* **17**, 6039 (1984).

⁴S. Datta and B. Das, *Appl. Phys. Lett.* **56**, 665 (1990).

⁵J. Nitta, F. E. Meijer, and H. Takayanagi, *Appl. Phys. Lett.* **75**, 695 (1999).

⁶T. Koga, J. Nitta, H. Takayanagi, and S. Datta, *Phys. Rev. Lett.* **88**, 126601 (2002).

⁷S. J. Gong and Z. Q. Yang, *J. Appl. Phys.* **102**, 033706 (2007).

⁸M. Z. Hasan and C. L. Kane, *Rev. Mod. Phys.* **82**, 3045 (2010).

⁹J. E. Hirsch, *Phys. Rev. Lett.* **83**, 1834 (1999).

¹⁰J. H. van Vleck, *Phys. Rev.* **52**, 1178 (1937).

¹¹J. Nitta, T. Akazaki, H. Takayanagi, and T. Enoki, *Phys. Rev. Lett.* **78**, 1335 (1997).

¹²S. LaShell, B. A. McDougall, and E. Jensen, *Phys. Rev. Lett.* **77**, 3419 (1996).

¹³G. Nicolay, F. Reinert, S. Hüfner, and P. Blaha, *Phys. Rev. B* **65**, 033407 (2001).

¹⁴Y. M. Koroteev, G. Bihlmayer, J. E. Gayone, E. V. Chulkov, S. Blügel, P. M. Echenique, and P. Hofmann, *Phys. Rev. Lett.* **93**, 046403 (2004).

¹⁵A. Varykhalov, D. Marchenko, M. R. Scholz, E. D. L. Rienks, T. K. Kim, G. Bihlmayer, J. Sánchez-Barriga, and O. Rader, *Phys. Rev. Lett.* **108**, 066804 (2012).

¹⁶O. Krupin, G. Bihlmayer, K. Starke, S. Gorovikov, J. E. Prieto, K. Döbrich, S. Blügel, and G. Kaindl, *Phys. Rev. B* **71**, 201403 (2005).

¹⁷B. Gu, I. Sugai, T. Ziman, G. Y. Guo, N. Nagaosa, T. Seki, K. Takanashi, and S. Maekawa, *Phys. Rev. Lett.* **105**, 216401 (2010).

¹⁸A. Nuber, J. Braun, F. Forster, J. Minár, F. Reinert, and H. Ebert, *Phys. Rev. B* **83**, 165401 (2011).

¹⁹A. Bendounan, K. Ait-Mansour, J. Braun, J. Minár, S. Bornemann, R. Fasel, O. Gröning, F. Sirotti, and H. Ebert, *Phys. Rev. B* **83**, 195427 (2011).

²⁰C. R. Ast, J. Henk, A. Ernst, L. Moreschini, M. C. Falub, D. Pacilé, P. Bruno, K. Kern, and M. Grioni, *Phys. Rev. Lett.* **98**, 186807 (2007).

²¹G. Bihlmayer, Y. M. Koroteev, P. M. Echenique, E. V. Chulkov, and S. Blügel, *Surf. Sci.* **600**, 3888 (2006).

²²S. R. Park, C. H. Kim, J. Yu, J. H. Han, and C. Kim, *Phys. Rev. Lett.* **107**, 156803 (2011).

²³C. G. Duan, J. P. Velez, R. F. Sabirianov, Z. Q. Zhu, J. H. Chu, S. S. Jaswal, and E. Y. Tsymbal, *Phys. Rev. Lett.* **101**, 137201 (2008).

²⁴G. Kresse and D. Joubert, *Phys. Rev. B* **59**, 1758 (1999).

²⁵S. Manne, H. J. Butt, S. A. C. Gould, and P. K. Hansma, *Appl. Phys. Lett.* **56**, 1758 (1990).

²⁶T. Kosugi, T. Miyake, and S. Ishibashi, *J. Phys. Soc. Jpn.* **80**, 074713 (2011).

²⁷S. Vajna, E. Simon, A. Szilva, K. Palotas, B. Ujfalussy, and L. Szunyogh, *Phys. Rev. B* **85**, 075404 (2012).

²⁸Y. K. Kato, R. C. Myers, A. C. Gossard, and D. D. Awschalom, *Science* **306**, 1910 (2004).

²⁹J. Yao and Z. Q. Yang, *Phys. Rev. B* **73**, 033314 (2006).

³⁰W. Yang and K. Chang, *Phys. Rev. B* **74**, 193314 (2006).

³¹J. Neugebauer and M. Scheffler, *Phys. Rev. B* **46**, 16067 (1992).

³²M. K. Niranjan, C. G. Duan, S. S. Jaswal, and E. Y. Tsymbal, *Appl. Phys. Lett.* **96**, 222504 (2010).

³³L. Petersen and P. Hedegård, *Surf. Sci.* **459**, 49 (2000).